

# Top quark flavor changing via photon

Sara Khatibi and Mojtaba Mohammadi Najafabadi

*School of Particles and Accelerators, Institute for Research in Fundamental Sciences (IPM) P.O. Box  
19395-5531, Tehran, Iran*

## Abstract

We present constraints on the top quark flavor changing neutral current in the vertices of  $tu\gamma$  and  $tc\gamma$  from the measured diphoton mass spectrum at the LHC. It is shown that the angular distributions of diphoton is highly affected by the anomalous  $tu\gamma$  and  $tc\gamma$  couplings at the LHC and can provide stringent limits on these couplings. We determine the constraints on the anomalous  $tu\gamma$  from the upper bound on the neutron electric dipole moment (EDM). It is found that the current upper limit on the neutron EDM excludes any value of the branching fraction of top quark rare decay to an up-quark plus a photon above  $2.04 \times 10^{-6}$ .

PACS Numbers: 13.66.-a, 14.65.Ha

**Keywords:** Top quark, photon, flavor changing neutral current.

# 1 Introduction

Study of the top quark properties is particularly interesting in searches for new physics as it couples strongly to the electroweak symmetry breaking sector because of its large mass. New physics can show up either through direct production of new particles or indirectly via higher order effects. Observing indirect evidences is important as it provides hints to look for new physics before direct discovery. In the Standard Model (SM), the branching fractions of top quark rare decays  $t \rightarrow qV$ , with  $q = u, c$  and  $V = \gamma, Z, g$ , are at the order of  $10^{-14} - 10^{-12}$  [1]. Such branching fractions are extremely small and are out of the ability of the current and future collider experiments to be measured. Within the SM, such Flavor Changing Neutral Current (FCNC) transitions only occur at loop level and are strongly suppressed due to the Glashow-Iliopoulos-Maiani (GIM) mechanism [2]. On the other hand, it has been shown that several extensions of the SM are able to relax the GIM suppression of the top quark FCNC transitions due to additional loop diagrams mediated by new particles. These models such as supersymmetry, Higgs doublet models predict significant enhancements for the FCNC top quark rare decays [3–17]. As a result, the observation of any excess for these rare decay would be indicative of indirect effects of new physics. Many studies on searches for the FCNC couplings have been already done [18–34].

In this paper, direct and indirect searches for the top quark FCNC interactions in the vertex of  $tq\gamma$  are discussed. Such interactions can be described in a model independent way using the effective Lagrangian approach, which has the following form [35]:

$$\mathcal{L}_{\text{FCNC}} = -eQ_t \sum_{q=u,c} \kappa_{tq\gamma} \bar{q}(\lambda_{tq\gamma}^v + \lambda_{tq\gamma}^a \gamma_5) \frac{i\sigma_{\mu\nu} q^\nu}{\Lambda} t A^\mu + h.c., \quad (1)$$

where the electric charges of the electron and top quark are denoted by  $e$  and  $Q_t$ , respectively and  $q^\nu$  is the four momentum of the involved photon,  $\Lambda$  is the cutoff of the effective theory, which is conventionally assumed to be equal to the top quark mass, unless we mention.  $P_L$  and  $P_R$  are the left-handed and right-handed projection operators and  $\sigma_{\mu\nu} = \frac{1}{2}[\gamma_\mu, \gamma_\nu]$ . The anomalous couplings strength is denoted by  $\kappa_{tq\gamma}$ . Throughout this paper, no specific chirality is assumed for the  $tq\gamma$  FCNC couplings, i.e.  $\lambda_{tq\gamma}^v = 1$  and  $\lambda_{tq\gamma}^a = 0$ . Within the SM framework, the values of  $\kappa_{tq\gamma}$ ,  $q = u, c$ , vanish at tree level.

The leading order (LO) partial width of the top quark FCNC decay  $t \rightarrow q\gamma$ , after neglecting the masses of the up and charm quarks, has the following form [36]:

$$\Gamma(t \rightarrow q\gamma) = \frac{\alpha}{2} Q_t^2 m_t |\kappa_{tq\gamma}|^2, \quad (2)$$

and the LO width of  $t \rightarrow bW^+$  can be written as [36, 37]:

$$\Gamma(t \rightarrow bW^+) = \frac{\alpha |V_{tb}|^2}{16s_W^2} \frac{m_t^3}{m_W^2} \left( 1 - \frac{3m_W^4}{m_t^4} + \frac{2m_W^6}{m_t^6} \right), \quad (3)$$

where  $\alpha$  and  $V_{tb}$  are the fine structure constant and the CKM matrix element, respectively. The sine of the Weinberg angle is denoted by  $s_W$  and  $m_t, m_W$  are the top quark and  $W$  boson mass, respectively. The branching fraction of  $t \rightarrow q\gamma$  is estimated as the ratio of  $\Gamma(t \rightarrow q\gamma)$  to the width of  $t \rightarrow bW^+$  which takes the following form [36]:

$$Br(t \rightarrow q\gamma) = 0.2058 \times |\kappa_{tq\gamma}|^2. \quad (4)$$

To obtain the above branching fraction, we set  $m_t = 172.5$  GeV,  $\alpha = 1/128.92$ ,  $m_W = 80.419$  GeV and  $s_W^2 = 0.234$  in  $t \rightarrow q\gamma$  and  $t \rightarrow bW^+$  widths.

The  $tu\gamma$  and  $tc\gamma$  FCNC couplings have been studied in different experiments with no observation of any excess above the SM expectation up to now. In  $p\bar{p}$  collisions at the Tevatron, the CDF experiment has set the following upper bounds on the branching fraction at 95% confidence level [38]:

$$Br(t \rightarrow q\gamma) < 3.2 \times 10^{-2}, \text{ with } q = u, c. \quad (5)$$

This upper bound has been obtained using the study of the top quark decays in top pair production at the Tevatron. There are also searches for the anomalous  $tq\gamma$  couplings in the electron-positron and electron-proton colliders which have provided the following limits on the anomalous couplings at 95% CL [39–41]:

$$\kappa_{tc\gamma} < 0.486 \text{ (DELPHI)}, \quad \kappa_{tu\gamma} < 0.174 \text{ (ZEUS)}, \quad \kappa_{tu\gamma} < 0.18 \text{ (H1)}. \quad (6)$$

These limits have been obtained in searches for anomalous single top quark production events at LEP and HERA. The ZEUS limit has been obtained under the assumption of  $m_t = 175$  GeV.

The most stringent bounds on the  $tq\gamma$  FCNC interactions are coming from the CMS experiment in proton-proton collisions at the LHC at the center-of-mass energy of 8 TeV by studying the final state of single top quark production in association with a photon. The following upper bounds have been obtained on the anomalous couplings and the corresponding branching fractions at 95% CL [42]:

$$\begin{aligned} \kappa_{tu\gamma} &< 0.028, \text{ corresponding to } Br(t \rightarrow u\gamma) < 1.61 \times 10^{-4}, \\ \kappa_{tc\gamma} &< 0.094, \text{ corresponding to } Br(t \rightarrow c\gamma) < 1.82 \times 10^{-3}. \end{aligned} \quad (7)$$

These limits have been obtained based on  $19.1 \text{ fb}^{-1}$  of integrated luminosity of data using only muonic decay mode of the W boson in the top quark decay.

All the above searches are based on the final states containing at least a top quark. As top quark has a short life time, it decays immediately (before hadronization) and therefore one has to reconstruct top quark from its decay products to be able to probe the  $tq\gamma$  couplings. This needs a careful attention to correctly select the final state objects, i.e. top quark decay products, and consider several sources of systematic uncertainties associated to each final state object in the detector. In this work, we propose to use diphoton events to probe the  $tq\gamma$  FCNC couplings which have less difficulties and challenges with respect to the events with top quarks in the final state.

Measurement of diphoton spectrum is one of the particular interests at the LHC as it is sensitive to several new physics models beyond the SM [43–46], and diphoton is the most promising channel in searching for the Higgs boson. On the other hand, the excellent mass resolution of the ATLAS and CMS detectors at the LHC provides the possibility for precise measurement of new signals above the SM expectation. Randall-Sundrum model and large extra dimensions are of the examples of the models which affect the diphoton differential cross sections. In this paper, we show that the presence of the FCNC anomalous coupling  $tq\gamma$  leads to significant change in the diphoton mass spectrum and the diphoton angular distribution. Using the current mass spectrum measurement by the CMS experiment [43], we obtain bounds on the anomalous couplings  $\kappa_{tq\gamma}$ . Then, it will be shown that diphoton angular distribution would be able to constrain the  $tq\gamma$  FCNC couplings strongly.

The anomalous  $tq\gamma$  coupling can also be studied indirectly via its effects in higher-order calculations such as the branching fraction of the bottom quark rare decay  $b \rightarrow s + \gamma$  [47]. As another indirect way to probe the FCNC couplings, we calculate the effect of  $tu\gamma$  coupling to the

neutron electric dipole moment (EDM) and show that the neutron EDM can receive significant contribution from the FCNC couplings. Using the upper bounds on the neutron EDM, upper limits on the anomalous  $tu\gamma$  is derived.

This paper is organized as follows. In Section 2, the details of the calculations and methods to constrain the  $tq\gamma$  FCNC couplings using the differential diphoton cross sections are presented. Section 3 is dedicated to present the calculations of the  $tu\gamma$  contribution to the neutron EDM and extract the upper bounds on  $\kappa_{tu\gamma}$ . Finally, Section 4 concludes the paper.

## 2 Diphoton analysis

In this section, we calculate the contribution of  $tq\gamma$  FCNC couplings to diphoton production at the LHC. Then, based on the measured diphoton mass spectrum by the CMS experiment [43], constraints on the anomalous couplings are derived.

Within the SM, the leading order diphoton production proceeds through quark-antiquark annihilation. The  $tq\gamma$  FCNC couplings affect the diphoton production through the scattering of  $u, c, \bar{u}$ , and  $\bar{c}$  quarks which proceed through  $t$ -channel as shown in Fig. 1.

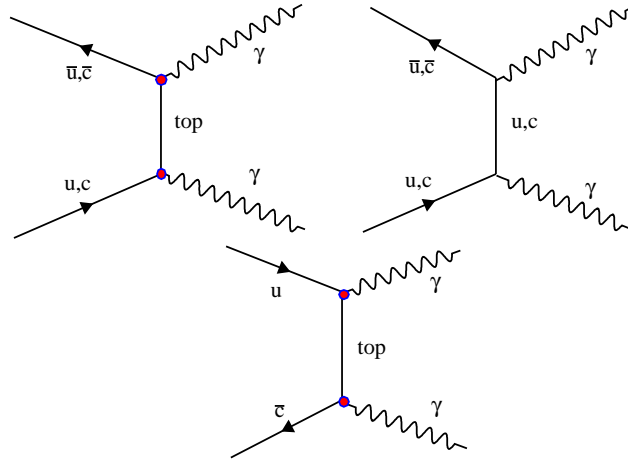


Figure 1: The representative Feynman diagrams of the  $tq\gamma$  FCNC contributions to the diphoton production at the LHC. The right diagram on the top represents the lowest order SM contribution to diphoton production which interfere with diagrams from  $tq\gamma$ .

We calculate the leading order matrix element of diphoton production analytically for the Feynman diagrams shown in Fig.1. After averaging over the color and spin indices of the initial state partons and summing over the polarizations of the final state photons, the amplitude takes the following form:

$$|\overline{\mathcal{M}}|^2 \propto \frac{2e^4 u}{t} + \frac{Q_t^2 e^4 \kappa^2 t(u - 4t)}{m_t^2(t - m_t^2)} + \frac{2Q_t^4 e^4 \kappa^4 t^2(m_t^2 s + tu)}{m_t^4(t - m_t^2)^2}, \quad (8)$$

where for simplicity, we have assumed  $\kappa_{tu\gamma} = \kappa_{tc\gamma} = \kappa$  and  $s, t, u$  are the Mandelstam variables which can be written in terms of the scattering angle  $\theta^*$  in the center-of-mass frame as:  $t =$

$-\frac{1}{2}(1 - \cos \theta^*)$  and  $u = -\frac{1}{2}(1 + \cos \theta^*)$ . The first term in the above expression is the leading order amplitude describing the SM diphoton production of  $q\bar{q} \rightarrow \gamma\gamma$ , the second term is the interference between the SM and FCNC diagram, and the last term is the contribution of pure  $tq\gamma$  FCNC diphoton production. One of the characteristics of the leading order SM is the enhancement of diphoton production at small angles as the production proceed through  $t$ -channel.

In order to perform the signal simulation, the  $tq\gamma$  effective Lagrangian, Eq.1, is implemented into the FEYNRULES package [48] and then the model is exported to a UFO module [49] which is linked to MADGRAPH 5 [50]. Then, we generate events describing the diphoton production at the LHC with the center-of-mass energy of  $\sqrt{s} = 8$  TeV. The leading order parton distribution functions (PDFs) of CTEQ6L1 [52] is used as the input for the calculations and events generation. PYTHIA 8 [53] is used for parton showering and hadronization of the parton level events. Finally, the effects of detector are accounted for using the recent version of DELPHES package [54]. It includes a reasonable modeling of the CMS detector performances as described in Ref. [55].

As we mentioned before, diphoton production at the LHC is one of the important final states to look for with a special attention as it is sensitive to new physics models beyond the SM and also it is the golden channel in searching for the Higgs boson. In [43], the CMS collaboration has performed a search for diphoton resonances in high mass in proton-proton collisions at the center-of-mass energy of 8 TeV using an integrated luminosity of  $19.5 \text{ fb}^{-1}$  of data. The analysis is to look for any resonances of the gravitons in the Randall-Sundrum scenario with a warped extra dimension. According to above calculations, the  $tq\gamma$  FCNC couplings affect the production of diphoton at the LHC. In this work, we follow the quite similar strategy to the CMS collaboration and use their result to probe the  $tq\gamma$  FCNC anomalous couplings.

In the CMS experiment analysis, two isolated photons with transverse energy ( $E_T$ ) greater than 80 GeV within the pseudorapidity range of  $|\eta_\gamma| < 1.4442$ , and with the diphoton invariant mass greater than 300 GeV are selected. In this region of the pseudorapidity, an excellent resolution for the photon energy is accessible. For the photons with  $E_T \sim 60$  GeV and  $|\eta| < 1.4442$ , the energy resolution varies between 1% – 3% [56]. The used cuts for isolation and identification of the photons by the CMS collaboration lead to an efficiency of 86% for the photons with  $E_T > 80$  GeV and  $|\eta_\gamma| < 1.4442$ . Small changes are seen in this efficiency when  $E_T$  and  $\eta$  of the photons change. In the current work, quite similar selection is employed for the analysis [43, 44].

The background to the diphoton final state originates from SM diphoton production,  $\gamma$ +jet, and from dijet productions where one or two jets are misidentified as photons in the detector for the latter two background processes. Table 1 shows the number of observed events in data and the background prediction for several ranges of the diphoton mass spectrum [43]. The uncertainties presented in the Table 1 include both the statistical and systematic sources. As it can be seen, the data and SM background expectation are in an overall agreement, considering the uncertainties on the predicted background and no significant excess over the SM background is found.

We use the CMS experiment measurement of diphoton spectrum presented in Table 1 to probe the  $tq\gamma$  anomalous couplings. As the measurement is compatible with the SM prediction, we set upper limit on the diphoton production cross section in the presence of the anomalous couplings. Figure 2 shows the diphoton mass distribution for the SM and SM+FCNC signal assuming  $\kappa_{tu\gamma} = \kappa_{tc\gamma} = \kappa = 0.1$ . As can be seen, the presence of  $tq\gamma$  FCNC couplings lead to increase the diphoton cross section in the high invariant mass region. According to Table 1, the total number of observed data events above  $m_{\gamma\gamma} > 500$  GeV is 333 events with the SM background prediction of  $375.8 \pm 29.9$  [43]. Assuming  $\kappa_{tu\gamma} = \kappa_{tc\gamma} = \kappa = 0.15$ , 99.4 FCNC events are expected in this region with an integrated luminosity of  $19.5 \text{ fb}^{-1}$  of data.

We proceed to set upper limit on the diphoton cross section in the presence of FCNC couplings.

Table 1: Number of observed events in data and the SM background prediction in different ranges of diphoton invariant mass with  $19.5 \text{ fb}^{-1}$  of data [43].

$m_{\gamma\gamma}$	Data	Total backgrounds	Uncertainty on bkg.
500-750 GeV	265	310.8	$\pm 29.9$
750-1000 GeV	46	48.6	$\pm 5.4$
1000-1250 GeV	16	11.4	$\pm 1.5$
1250-1500 GeV	3	3.3	$\pm 0.5$
1500-1750 GeV	2	1.1	$\pm 0.2$
1750- $\infty$ GeV	1	0.6	$\pm 0.1$

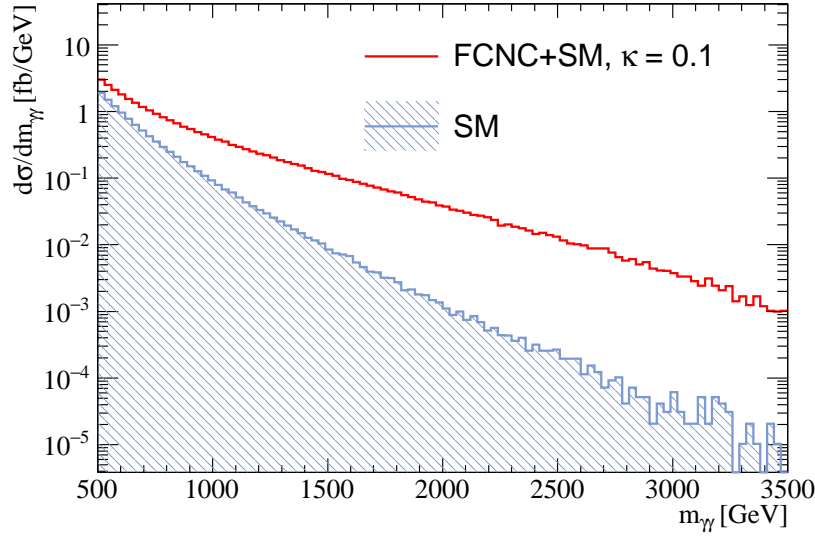


Figure 2: Diphoton invariant mass distribution for SM and SM+FCNC with  $\kappa = 0.1$ .

We compare the number of observed events in data and the expected events from SM in the region  $m_{\gamma\gamma} > 500 \text{ GeV}$ . Upper limit at 95% CL is set on the quantity  $\sigma_s = (\sigma_{\text{Total}} - \sigma_{\text{SM}}) \times \epsilon_A$ , where the whole diphoton production cross section (SM and FCNC signal) is denoted by  $\sigma_{\text{Total}}$  and  $\sigma_{\text{SM}}$  is the SM diphoton cross section. The FCNC signal acceptance is shown by  $\epsilon_A$ . The  $\text{CL}_s$  technique [57] is used to calculate the upper limit on the cross section. An efficiency of 77.45% with an uncertainty of 10% is found for the FCNC signal. The observed and expected 95% CL upper limit on  $\sigma_s$  are found to be 3.2 fb and 5.0 fb. The observed limit at 95% CL and the FCNC signal cross section,  $\sigma_s$  are shown in Fig. 3.

The 95% CL upper limit on the anomalous coupling parameter  $\kappa$  is the intersection of the observed limit on cross section with the theoretical cross section curve. The upper limit on  $\sigma_s$  (3.2 fb) is corresponding to the upper limit of 0.153 on the anomalous coupling  $\kappa$ . This limit can be expressed to the upper limit on the branching fraction using Eq.4:

$$\text{Br}(t \rightarrow q\gamma) < 4.81 \times 10^{-3}, \text{ with } q = u, c. \quad (9)$$

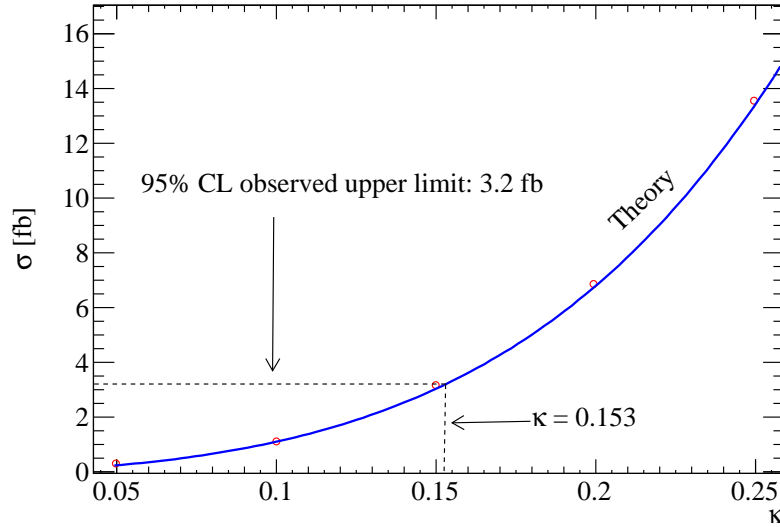


Figure 3: Parameterization of signal cross section versus the anomalous FCNC coupling  $\kappa$  and the 95% observed upper limit on the cross section.

This limit is comparable with the most stringent limits which has been obtained from the anomalous single top quark production in association with a photon by the CMS experiment (Eq.7) [42]. It should be mentioned that in this analysis leading order cross section for the signal has been used however, including the higher order effects would improve the limits.

## 2.1 Diphoton angular distribution

In this section, we propose and use a diphoton angular variable to probe the  $tq\gamma$  anomalous couplings. In the SM, as the diphoton production proceeds through  $t$ -channel, the angular distribution peaks at  $\cos\theta^* = 1$ , where  $\theta^*$  is the scattering angle in the center-of-mass frame of two partons. The scattering angle between two photons can be expressed by the variable  $\chi = e^{|\eta_{\gamma_1} - \eta_{\gamma_2}|}$ . This variable has been used widely in searches for new physics such as searches for contact interactions, large extra dimensions, and excited quarks in dijet events in the Tevatron and LHC experiments [58–61]. It has been found that new phenomena affect this angular variable considerably and consequently is used to probe beyond SM.

The left plot in Fig. 4 shows the distributions of  $\chi = e^{|\eta_{\gamma_1} - \eta_{\gamma_2}|}$  as a function of the anomalous coupling  $\kappa$ . The distribution is normalized to unity since the sensitivity to FCNC couplings affects the angular distribution rather than normalization. This figure depicts the predicted SM distribution as well as the SM+FCNC with  $\kappa = 0.1, 0.2$  and  $0.5$ . These distributions are after all selection cuts described previously and with  $m_{\gamma\gamma} > 500$  GeV. As seen, the presence of the anomalous FCNC couplings of  $tq\gamma$  changes the shape of the angular variable  $\chi$ . Increasing the value of the anomalous coupling  $\kappa$  causes more events to be concentrated at small values of  $\chi$ . It is notable that due to the detector acceptance cut applied on the photon pseudorapidity,  $\chi$  varies from 0 to  $e^{2 \times 1.442} = 17.96$ .

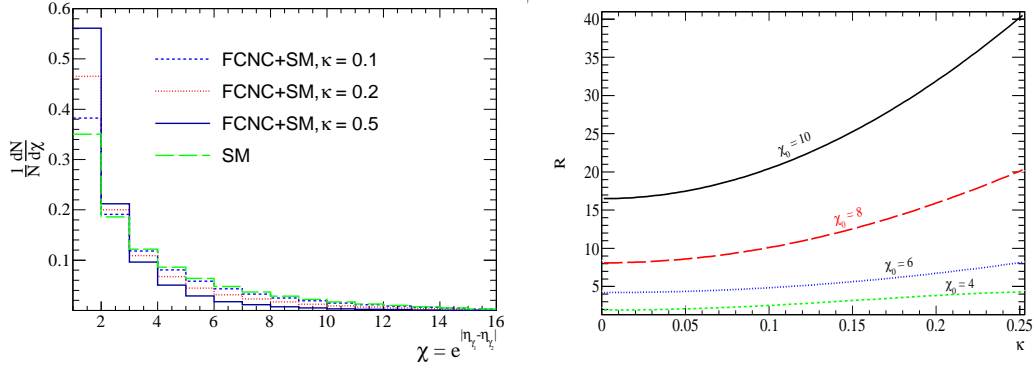


Figure 4: Left: Normalized distributions of diphoton angular variable  $\chi$  for the SM and SM+FCNC with anomalous couplings  $\kappa = 0.1, 0.2, 0.5$ . Right:  $\mathcal{R}$  versus the anomalous coupling  $\kappa$  for various choices of  $\chi_0$ .

In order to quantify the difference in the shape of  $\chi$  for SM and FCNC, a ratio is defined as:

$$\mathcal{R}_{\chi_0}(\kappa) = \frac{\int_0^{\chi_0} \frac{1}{N} \frac{dN}{d\chi}}{\int_{\chi_0}^{\infty} \frac{1}{N} \frac{dN}{d\chi}}, \quad (10)$$

where  $\chi_0$  is an arbitrary cut which is chosen in such a way that the best sensitivity to the FCNC couplings is achieved. The right plot in Fig. 4 shows the behavior of  $\mathcal{R}$  versus the anomalous coupling  $\kappa$  for different choices of  $\chi_0$ . As the normalized distribution of  $\chi$  depends on the cut on the diphoton invariant mass, the value of  $\mathcal{R}$  varies with the cut on  $m_{\gamma\gamma}$ . Figure 5 shows the behavior of  $\mathcal{R}$  for the SM and SM+FCNC with for example the choice of  $\chi_0 = 8$  in terms of cut on the diphoton invariant mass. The uncertainties in this plot includes only the theoretical uncertainties arising from variation of factorization and renormalization scales and the uncertainty due to the choice of PDF. The uncertainty coming from limited knowledge on the choice of PDF is obtained using PDF4LHC recommendation [62, 63]. The cut on  $m_{\gamma\gamma}$  can be chosen to optimize the expected sensitivity to the model parameter, i.e.  $\kappa$ .

We define the statistical significance of observable  $\mathcal{R}$  as:

$$\mathcal{S}_{\chi_0}(\kappa) = \frac{\mathcal{R}_{\chi_0}^{\text{FCNC+SM}}(\kappa) - \mathcal{R}_{\chi_0}^{\text{SM}}}{\Delta \mathcal{R}_{\chi_0}^{\text{SM}}}, \quad (11)$$

where  $\mathcal{R}_{\chi_0}^{\text{SM}}$  and  $\mathcal{R}_{\chi_0}^{\text{FCNC+SM}}$  are the values of the ratio defined in Eq.10 with a choice of  $\chi_0$  for the SM and for the case of the presence of FCNC. The uncertainty on  $\mathcal{R}_{\chi_0}^{\text{SM}}$  is denoted by  $\Delta \mathcal{R}_{\chi_0}^{\text{SM}}$ . Considering the theoretical and statistical uncertainties in the region of  $m_{\gamma\gamma} > 500$ , the value of  $\chi_0 = 8$  provides the best sensitivity. The  $1\sigma$  and  $2\sigma$  regions of the FCNC anomalous coupling are found to be:

$$\begin{aligned} 1\sigma : \kappa &< 4.0 \times 10^{-2} \text{ corresponding to } Br(t \rightarrow q\gamma) < 3.31 \times 10^{-4}, \\ 2\sigma : \kappa &< 5.6 \times 10^{-2} \text{ corresponding to } Br(t \rightarrow q\gamma) < 6.46 \times 10^{-4}. \end{aligned} \quad (12)$$

As can be seen, the angular variable  $\chi$  is able to provide better sensitivity to the anomalous couplings with respect to the diphoton mass spectrum with one order of magnitude. To achieve a better sensitivity, the optimization can be done on both  $\chi_0$  and cut on the  $m_{\gamma\gamma}$ . It is notable that



the QCD and electroweak higher order corrections may modify the shape of  $\chi$  variable distribution which needs to be considered in a detailed analysis and is beyond the scope of this work.

At the end of this section, it is worth mentioning that similar to above analysis, the measured differential distributions of dijet events by the LHC experiments can also be used to probe the FCNC interactions of  $tqg$  [58].

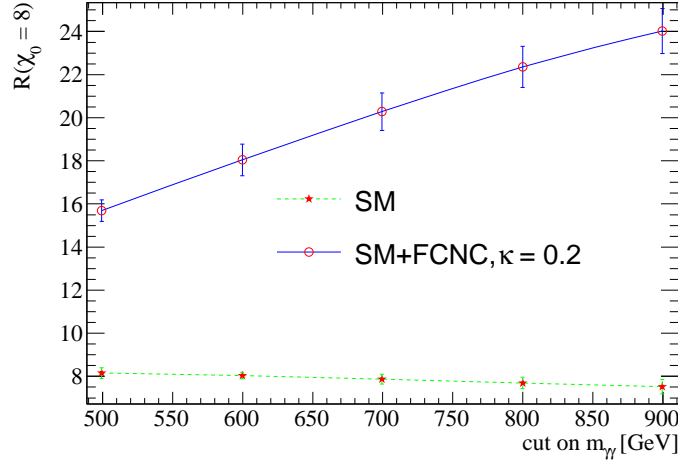


Figure 5: The behavior of  $\mathcal{R}$  in terms of the cut on diphoton mass for the SM and SM+FCNC at  $\chi_0 = 8$  and with the choice of  $\kappa = 0.2$ .

### 3 Electric dipole moment analysis

In this section, we obtain upper limit on the  $tu\gamma$  FCNC coupling using the present upper bound on the neutron electric dipole moment. Such an approach has been used in constraining the  $W$  boson electric dipole moment [64], top-Higgs non-standard interactions [65], and probing heavy charged gauge boson mass and couplings [66].

We calculate the contribution of the  $tu\gamma$  coupling to the neutron EDM using the effective interaction for the  $q\bar{q}\gamma$  vertex. The most general effective vertex describing the interaction of a photon with two on-shell quarks can be written as [35]:

$$\Gamma_\mu(q^2) = -ie \left( \gamma_\mu F_{1v}(q^2) + \frac{\sigma_{\mu\nu}}{2m_q} q^\nu [iF_{2v}(q^2) + F_{2a}(q^2)\gamma_5] \right), \quad (13)$$

where  $q$  is the four-momentum of the off-shell photon. The functions  $F_{1v}(q^2)$  and  $F_{2v,2a}(q^2)$  are called form factors which in the low energy limit  $q^2 \rightarrow 0$ , they are physical parameters and be related to the static physical quantities according to the following relations:

$$F_{1v}(0) = Q_q, \quad F_{2v}(0) = a_q, \quad F_{2a} = d_q \frac{2m_q}{e}, \quad (14)$$

where  $Q_q$  is the electric charge of a quark  $q$ ,  $a_q$  and  $d_q$  are the magnetic dipole moment and electric dipole moment of a quark. The electric dipole moment term violates the P and CP

invariance. Within the SM at tree level,  $d_q$  and  $a_q$  are zero and however non-zero values for  $d_q$  and  $a_q$  arise from higher order corrections. The SM prediction for the electric dipole moments of the quarks are extremely small and expected to be smaller  $10^{-30}$  e.cm [67–70].

Using the interactions described by Eq.13 at low energy, the  $tu\gamma$  FCNC coupling introduced by Eq.1, the induced CP violating amplitude coming from the  $tu\gamma$  FCNC interaction in Fig. 6 can be expressed as:

$$\Gamma_\mu = \bar{u}(p_2) \left[ \int \frac{d^4 k}{(2\pi)^4} \left( \frac{Q_t e \kappa_{tu\gamma}}{\Lambda} \sigma_{\beta\beta'} k^{\beta'} \right) \frac{i(\not{k} - \not{p}_2 + m_t)}{(k - p_2)^2 - m_t^2} (-i d_t \gamma_5 \sigma_{\mu\nu} q^\nu) \frac{i(\not{k} - \not{p}_1 + m_t)}{(k - p_1)^2 - m_t^2} \left( \frac{Q_t e \kappa_{tu\gamma}}{\Lambda} \sigma_{\alpha\alpha'} k^{\alpha'} \right) \frac{-i g^{\alpha\beta}}{k^2} \right] u(p_1). \quad (15)$$

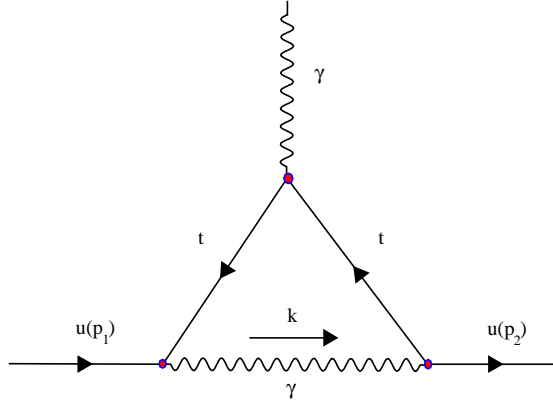


Figure 6: Feynman diagram contributing to the on shell  $u\bar{u}\gamma$  vertex originating from the  $tuH$  interaction.

After employing Dirac equation and Gordon identity, the above expression can be simplified to find the up quark EDM arising from  $tu\gamma$  FCNC coupling, which is the coefficient of  $\sigma_{\mu\nu} q^\nu \gamma_5$ . This integral on  $k$  is divergent, therefore a mass scale of  $\Lambda_{cut}$  is introduced as an ultraviolet cutoff scale. After performing some algebraic manipulations and integration over  $k$ , the amplitude is found to be:

$$\begin{aligned} \Gamma_\mu &= \frac{d_t \left( \frac{Q_t e \kappa_{tu\gamma}}{\Lambda} \right)^2 m_t^2}{(4\pi)^2} [\bar{u}(p_2) i \gamma_5 \sigma_{\mu\nu} q^\nu u(p_1)] \int 2dx dy \\ &\times \left\{ \frac{-\Lambda_{cut}^2}{m_t^2} + \ln \frac{\Lambda_{cut}^2}{\Delta} [6x_u(x+y)(x+y-1) + 3(x+y) + x_u - 1] + \frac{x_u(x+y)}{2(1+x_u(x+y-1))} \right\}, \end{aligned} \quad (16)$$

where  $d_t$  is the top quark EDM and

$$\Delta = m_t^2(x+y)[1+x_u(x+y-1)], \quad x_u = \frac{m_u^2}{m_t^2}.$$

As  $x_u \sim 10^{-5}$ , we take the limit of the amplitude for the case of  $x_u \rightarrow 0$ . We find the following form for the amplitude:

$$\Gamma_\mu = \frac{d_t e^2 Q_t^2 \kappa_{tu\gamma}^2 m_t^2}{(4\pi)^2 \Lambda^2} [\bar{u}(p_2) i \gamma_5 \sigma_{\mu\nu} q^\nu u(p_1)] \left\{ \frac{1}{6} - \frac{\Lambda_{cut}^2}{m_t^2} + \ln \frac{\Lambda_{cut}^2}{m_t^2} \right\}. \quad (17)$$

Employing the effective coupling for  $u\bar{u}\gamma$  coupling, we find the  $tu\gamma$  contribution to the up quark EDM:

$$d_u = \frac{d_t e^2 Q_t^2 \kappa_{tu\gamma}^2 m_t^2}{(4\pi)^2 \Lambda^2} \left\{ \frac{1}{6} - \frac{\Lambda_{\text{cut}}^2}{m_t^2} + \ln \frac{\Lambda_{\text{cut}}^2}{m_t^2} \right\}. \quad (18)$$

As seen, there are quadratic and logarithmic divergences to the up quark EDM from  $tu\gamma$  FCNC. However, there is a factor  $\Lambda^2$  in the denominator which comes from the  $tu\gamma$  effective coupling and is the scale at which new physics effects are expected to appear. It is natural to assume that the cutoff scale of the loop divergences ( $\Lambda_{\text{cut}}$ ) is equal to  $\Lambda$  which is the scale at which new physics effects are expected to show up, i.e.  $\Lambda_{\text{cut}} = \Lambda$ .

Using the non-relativistic SU(6) wave functions, the neutron EDM can be related to the up and down quark EDMs. The neutron EDM in terms of EDMs of quarks is written as [70]:

$$d_n = \eta \left( \frac{4}{3} d_d - \frac{1}{3} d_u \right), \quad (19)$$

where the up and down quarks EDMs are denoted by  $d_u$  and  $d_d$  and  $\eta$  describes the QCD higher order corrections and is equal to 0.61. The current experimental bound on the neutron EDM is  $d_n < 2.9 \times 10^{-26}$  e.cm. [71, 72]. The measured upper limit on the top quark EDM has been found to be  $d_t < 10^{-16}$  e.cm [73]. These upper limits lead to the allowed region for the  $tu\gamma$  FCNC coupling  $\kappa_{tu\gamma}$  and the new physics scale  $\Lambda$  which is presented in Fig. 7. According to Fig. 7, the maximum allowed value for  $\kappa_{tu\gamma}$  is 0.00315 which is corresponding to an energy scale close to the top quark mass.

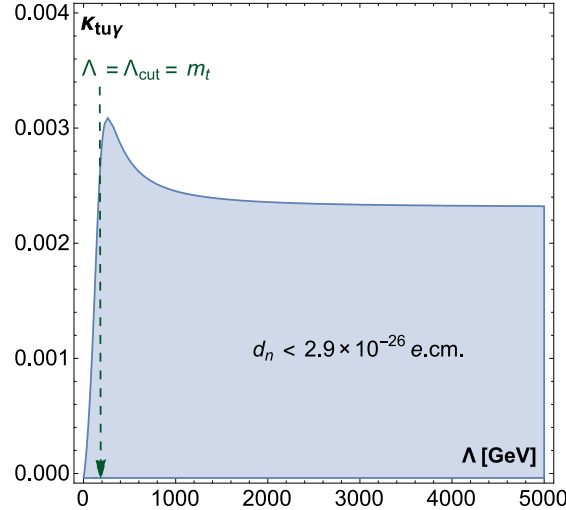


Figure 7: The 95% CL allowed region of  $\kappa_{tu\gamma}, \Lambda$  using the upper limit on the neutron EDM.

As  $\Lambda \rightarrow \infty$ , the allowed value for  $\kappa_{tu\gamma} \rightarrow 0.00237$ . Using the largest allowed value for  $\kappa_{tu\gamma}$ , 0.00315, the following upper limit from neutron EDM is obtained on the branching fraction of  $t \rightarrow u\gamma$ :

$$Br(t \rightarrow u\gamma) < 2.04 \times 10^{-6}. \quad (20)$$

This limit is two orders of magnitude tighter than the limits obtained from CMS experiment direct searches, mentioned in Eq.7.

## 4 Summary and conclusions

Rare top quark decays through flavor changing neutral currents in the vertices of  $tq\gamma$ ,  $tqZ$ , and  $tqg$  are particularly interesting as they are significantly sensitive to many extensions of the SM. The SM predictions for these rare decay modes are unobservably small (less than  $10^{-12}$ ) while new physics models are able to enhance the branching fractions by several order of magnitudes. As a results, any observation of such processes would indicate new physics beyond the SM. In this paper, we propose new direct and indirect ways to search for the  $tu\gamma$  and  $tc\gamma$  FCNC interactions. So far, these couplings have been directly studied by CDF, DELPHI, H1, ZEUS, and CMS experiments at colliders with at least a top quark in the final state of the collisions. In this work, we propose to use the diphoton differential distributions, mass and angular, to probe the  $tq\gamma$  FCNC couplings. Using the current measured mass spectrum of diphoton at the LHC with the CMS experiment, an upper limit of  $4.81 \times 10^{-3}$  is set on the branching fraction of  $t \rightarrow q\gamma$ . We show that the angular variable  $\chi = e^{|\eta_{\gamma 1} - \eta_{\gamma 2}|}$  would allow us to probe this branching fraction down to  $6.46 \times 10^{-4}$ . Such limits are much better than the previous experiments and are comparable with the ones obtained recently from anomalous single top events by the CMS experiment. As an indirect search, we calculate the contribution of the  $tu\gamma$  FCNC coupling to the neutron EDM and using the current upper limit on the neutron EDM, an upper limit on the branching fraction of  $t \rightarrow u\gamma$  is derived. The limit is found to be  $2.04 \times 10^{-6}$  which is two order of magnitude tighter than the ones from collider experiments.

## References

- [1] J. A. Aguilar-Saavedra and B. M. Nobre, Phys. Lett. B **553**, 251 (2003) [hep-ph/0210360].
- [2] S. L. Glashow, J. Iliopoulos and L. Maiani, Phys. Rev. D **2**, 1285 (1970).
- [3] G. Eilam, J. L. Hewett and A. Soni, Phys. Rev. D **44**, 1473 (1991) [Phys. Rev. D **59**, 039901 (1999)].
- [4] F. del Aguila, J. A. Aguilar-Saavedra and R. Miquel, Phys. Rev. Lett. **82**, 1628 (1999) [hep-ph/9808400].
- [5] D. Atwood, L. Reina and A. Soni, Phys. Rev. D **55**, 3156 (1997) [hep-ph/9609279].
- [6] S. Bejar, hep-ph/0606138.
- [7] R. Gaitan, R. Martinez and J. H. M. de Oca, arXiv:1503.04391 [hep-ph].
- [8] G. Abbas, A. Celis, X. Q. Li, J. Lu and A. Pich, arXiv:1503.06423 [hep-ph].
- [9] B. Altunkaynak, W. S. Hou, C. Kao, M. Kohda and B. McCoy, arXiv:1506.00651 [hep-ph].
- [10] J. M. Yang, B. L. Young and X. Zhang, Phys. Rev. D **58**, 055001 (1998) [hep-ph/9705341].
- [11] G. M. de Divitiis, R. Petronzio and L. Silvestrini, Nucl. Phys. B **504**, 45 (1997) [hep-ph/9704244].
- [12] J. L. Lopez, D. V. Nanopoulos and R. Rangarajan, Phys. Rev. D **56**, 3100 (1997) [hep-ph/9702350].
- [13] J. Guasch and J. Sola, Nucl. Phys. B **562**, 3 (1999) [hep-ph/9906268].

- [14] J. J. Liu, C. S. Li, L. L. Yang and L. G. Jin, Phys. Lett. B **599**, 92 (2004) [hep-ph/0406155].
- [15] J. J. Cao, G. Eilam, M. Frank, K. Hikasa, G. L. Liu, I. Turan and J. M. Yang, Phys. Rev. D **75**, 075021 (2007) [hep-ph/0702264].
- [16] K. Agashe, G. Perez and A. Soni, Phys. Rev. D **75**, 015002 (2007) [hep-ph/0606293].
- [17] K. Agashe and R. Contino, Phys. Rev. D **80**, 075016 (2009) [arXiv:0906.1542 [hep-ph]].
- [18] R. Goldouzian, Phys. Rev. D **91**, no. 1, 014022 (2015) [arXiv:1408.0493 [hep-ph]].
- [19] J. A. Aguilar-Saavedra and G. C. Branco, Phys. Lett. B **495**, 347 (2000) [hep-ph/0004190].
- [20] G. Durieux, F. Maltoni and C. Zhang, Phys. Rev. D **91**, no. 7, 074017 (2015) [arXiv:1412.7166 [hep-ph]].
- [21] S. Khatibi and M. M. Najafabadi, Phys. Rev. D **89**, no. 5, 054011 (2014) [arXiv:1402.3073 [hep-ph]].
- [22] J. L. Agram, J. Andrea, E. Conte, B. Fuks, D. Gel and P. Lansonneur, Phys. Lett. B **725**, 123 (2013) [arXiv:1304.5551 [hep-ph]].
- [23] J. A. Aguilar-Saavedra, Nucl. Phys. B **837**, 122 (2010) [arXiv:1003.3173 [hep-ph]].
- [24] F. Larios, R. Martinez and M. A. Perez, Phys. Rev. D **72**, 057504 (2005) [hep-ph/0412222].
- [25] H. Hesari, H. Khanpour, M. K. Yanehsari and M. M. Najafabadi, Adv. High Energy Phys. **2014**, 476490 (2014) [arXiv:1412.8572 [hep-ex]].
- [26] H. Hesari, H. Khanpour and M. M. Najafabadi, arXiv:1508.07579 [hep-ph].
- [27] H. Khanpour, S. Khatibi, M. K. Yanehsari and M. M. Najafabadi, arXiv:1408.2090 [hep-ph].
- [28] N. Craig, J. A. Evans, R. Gray, M. Park, S. Somalwar, S. Thomas and M. Walker, Phys. Rev. D **86**, 075002 (2012) [arXiv:1207.6794 [hep-ph]].
- [29] S. M. Etesami and M. Mohammadi Najafabadi, Phys. Rev. D **81**, 117502 (2010) [arXiv:1006.1717 [hep-ph]].
- [30] D. Kim and M. Park, arXiv:1507.03990 [hep-ph].
- [31] J. Cao, C. Han, L. Wu, J. M. Yang and M. Zhang, Eur. Phys. J. C **74**, no. 9, 3058 (2014) [arXiv:1404.1241 [hep-ph]].
- [32] A. Arhrib, R. Benbrik, C. H. Chen, M. Gomez-Bock and S. Semlali, arXiv:1508.06490 [hep-ph].
- [33] A. Greljo, J. F. Kamenik and J. Kopp, JHEP **1407**, 046 (2014) [arXiv:1404.1278 [hep-ph]].
- [34] C. Degrande, F. Maltoni, J. Wang and C. Zhang, Phys. Rev. D **91**, 034024 (2015) [arXiv:1412.5594 [hep-ph]].
- [35] J. A. Aguilar-Saavedra, Nucl. Phys. B **812**, 181 (2009) [arXiv:0811.3842 [hep-ph]].
- [36] J. A. Aguilar-Saavedra Acta Phys. Polon. **B35** 2695 (2004) [hep-ph/0409342].

- [37] M. Mohammadi Najafabadi, J. Phys. G **34**, 39 (2007) [hep-ph/0601155].
- [38] CDF Collaboration, Phys. Rev. Lett. **80**, 2525 (1998).
- [39] DELPHI Collaboration, Phys. Lett. **B 590**, 21 (2004) [hep-ex/0404014].
- [40] ZEUS Collaboration, Phys. Lett. **B559**, 153 (2003) [hep-ex/0302010].
- [41] H1 Collaboration, Phys. Lett. **B 678**, 450 (2009) [arXiv:0904.3876 [hep-ex]].
- [42] CMS Collaboration [CMS Collaboration], CMS-PAS-TOP-14-003.
- [43] CMS Collaboration [CMS Collaboration], CMS-PAS-EXO-12-045.
- [44] S. Chatrchyan *et al.* [CMS Collaboration], Phys. Rev. Lett. **108**, 111801 (2012) [arXiv:1112.0688 [hep-ex]].
- [45] G. Aad *et al.* [ATLAS Collaboration], Phys. Rev. D **92**, no. 3, 032004 (2015) [arXiv:1504.05511 [hep-ex]].
- [46] G. Aad *et al.* [ATLAS Collaboration], New J. Phys. **15**, 043007 (2013) [arXiv:1210.8389 [hep-ex]].
- [47] T. Han, K. Whisnant, B. L. Young and X. Zhang, Phys. Rev. D **55**, 7241 (1997) [hep-ph/9603247].
- [48] A. Alloul, N. D. Christensen, C. Degrande, C. Duhr and B. Fuks, Comput. Phys. Commun. **185**, 2250 (2014) [arXiv:1310.1921 [hep-ph]].
- [49] C. Degrande, C. Duhr, B. Fuks, D. Grellscheid, O. Mattelaer and T. Reiter, Comput. Phys. Commun. **183**, 1201 (2012) [arXiv:1108.2040 [hep-ph]].
- [50] J. Alwall, M. Herquet, F. Maltoni, O. Mattelaer and T. Stelzer, JHEP **1106**, 128 (2011) [arXiv:1106.0522 [hep-ph]].
- [51] J. Alwall *et al.*, JHEP **1407**, 079 (2014) [arXiv:1405.0301 [hep-ph]].
- [52] J. Pumplin, D. R. Stump, J. Huston, H. L. Lai, P. M. Nadolsky and W. K. Tung, JHEP **0207**, 012 (2002) [hep-ph/0201195].
- [53] T. Sjostrand, S. Mrenna and P. Z. Skands, Comput. Phys. Commun. **178**, 852 (2008) [arXiv:0710.3820 [hep-ph]].
- [54] J. de Favereau *et al.* [DELPHES 3 Collaboration], JHEP **1402**, 057 (2014) [arXiv:1307.6346 [hep-ex]].
- [55] S. Chatrchyan *et al.* [CMS Collaboration], JINST **3**, S08004 (2008).
- [56] V. Khachatryan *et al.* [CMS Collaboration], JINST **10**, no. 08, P08010 (2015) [arXiv:1502.02702 [physics.ins-det]].
- [57] A. L. Read, J. Phys. G **28**, 2693 (2002).
- [58] G. Aad *et al.* [ATLAS Collaboration], Phys. Rev. Lett. **114**, no. 22, 221802 (2015) [arXiv:1504.00357 [hep-ex]].

- [59] P. Meade and L. Randall, JHEP **0805**, 003 (2008) [arXiv:0708.3017 [hep-ph]].
- [60] L. A. Anchordoqui, J. L. Feng, H. Goldberg and A. D. Shapere, Phys. Lett. B **594**, 363 (2004) [hep-ph/0311365].
- [61] U. Baur, I. Hinchliffe and D. Zeppenfeld, Int. J. Mod. Phys. A **2**, 1285 (1987).
- [62] S. Alekhin *et al.*, arXiv:1101.0536 [hep-ph].
- [63] M. Botje *et al.*, arXiv:1101.0538 [hep-ph].
- [64] W. J. Marciano and A. Queijeiro, Phys. Rev. D **33**, 3449 (1986).
- [65] S. Khatibi and M. M. Najafabadi, Phys. Rev. D **90**, no. 7, 074014 (2014) [arXiv:1409.6553 [hep-ph]].
- [66] S. Y. Ayazi, S. Khatibi and M. Mohammadi Najafabadi, JHEP **1210**, 103 (2012) [arXiv:1205.3311 [hep-ph]].
- [67] A. Soni and R. M. Xu, Phys. Rev. Lett. **69**, 33 (1992).
- [68] W. Bernreuther, R. Bonciani, T. Gehrmann, R. Heinesch, T. Leineweber, P. Mastrolia and E. Remiddi, Phys. Rev. Lett. **95**, 261802 (2005) [hep-ph/0509341].
- [69] W. Bernreuther, R. Bonciani, T. Gehrmann, R. Heinesch, T. Leineweber and E. Remiddi, Nucl. Phys. B **723**, 91 (2005) [hep-ph/0504190].
- [70] M. Pospelov and A. Ritz, Annals Phys. **318**, 119 (2005) [hep-ph/0504231].
- [71] I. S. Altarev *et al.*, Phys. Lett. B **276**, 242 (1992).
- [72] I. S. Altarev *et al.*, Phys. Atom. Nucl. **59**, 1152 (1996) [Yad. Fiz. **59N7**, 1204 (1996)].
- [73] J. L. Hewett and T. G. Rizzo, Phys. Rev. D **49**, 319 (1994) [hep-ph/9305223].